Cells and cell culture

Three cell lines were used in this study PBT030, PBT138, HT1080. All cell lines were positive for IL13Rα2 and antigen level >80%. PBT138 and HT1080 was lentivirally modified to express varied levels of IL13Rα2. Initially PBT030 and PBT138 were seeded with both 12.5k and 25k cells to investigate effect of cell seeding on tumor cell proliferation. Later 12.5K were decided to seed to keep the system below confluency for longer time period. As HT1080 is a highly proliferative cell line, only 2K number of cells were seeded to keep the system below confluency.

Table S1: Cancer cell lines, CAR T-cells, seeding and effector to target ratios used in the *in vitro* experiments.

Tumor Cell Line	CAR T-cell	Tumor cell seeding	Effector : Target
PBT030	BBζ, 28ζ	12.5K, 25K	1:20, 1:10,1:5
PBT138-High	BBζ, 28ζ	12.5K, 25K,	1:20, 1:10, 1:5
HT1080-High, HT1080-Medium, HT1080-Low	BBζ, 28ζ	2K	1:20, 1:10, 1:5
PBT138-High, PBT138-Medium, PBT138-Low	BBζ, 28ζ	12.5K	1:20, 1:10, 1:5

SUPPLEMENTARY DATA 1 (Figs. S1-S7)
Data supporting CARRGO model assumptions

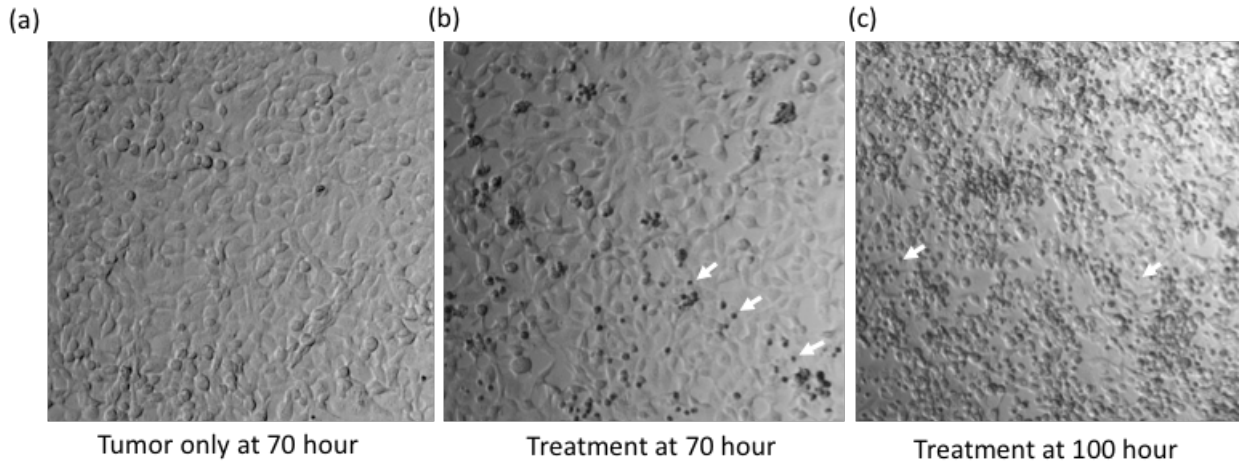

Figure S1. Well-mixed population. Microscopic images of HT1080-High IL13Rα2-expressing tumor only (a) at 70 hours post seeding during Logistic growth, and cancer cells with CAR T-cells (b) at 70 hours and (c) at 100 hours post seeding. White arrows indicate examples of CAR T-cells which appear as small dots as compared to the larger cancer cells. CAR T-cells are well-mixed with the cancer cell population. Both cancer cells and CAR T-cells are spread/attached on the bottom of the well. Because the CAR T-cells are small as compared to cancer cells, they contribute very little to the measured cell index.

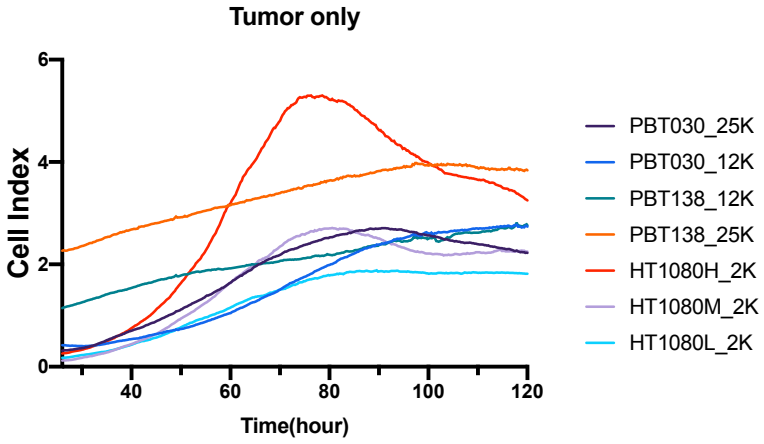

Figure S2. Logistic growth. Cancer cell dynamics of different cell lines at various seeding densities demonstrate logistic growth. Cancer cell lines shown here are only from the untreated wells and demonstrate that long-term growth dynamics are limited by physical and nutrient constraints of the system. We note that HT1080H,M reach confluency at approximately 80 hours post seeding. The linear relation between CI and cell number is lost after the cells reach confluency therefore we used only up to 80% of the confluency data in our CARRGO model fitting (c.f. Figure 2). PBT lines reached confluency at approximately 120 hours post seeding.

Raw xCELLigence data and CARRGO model fits

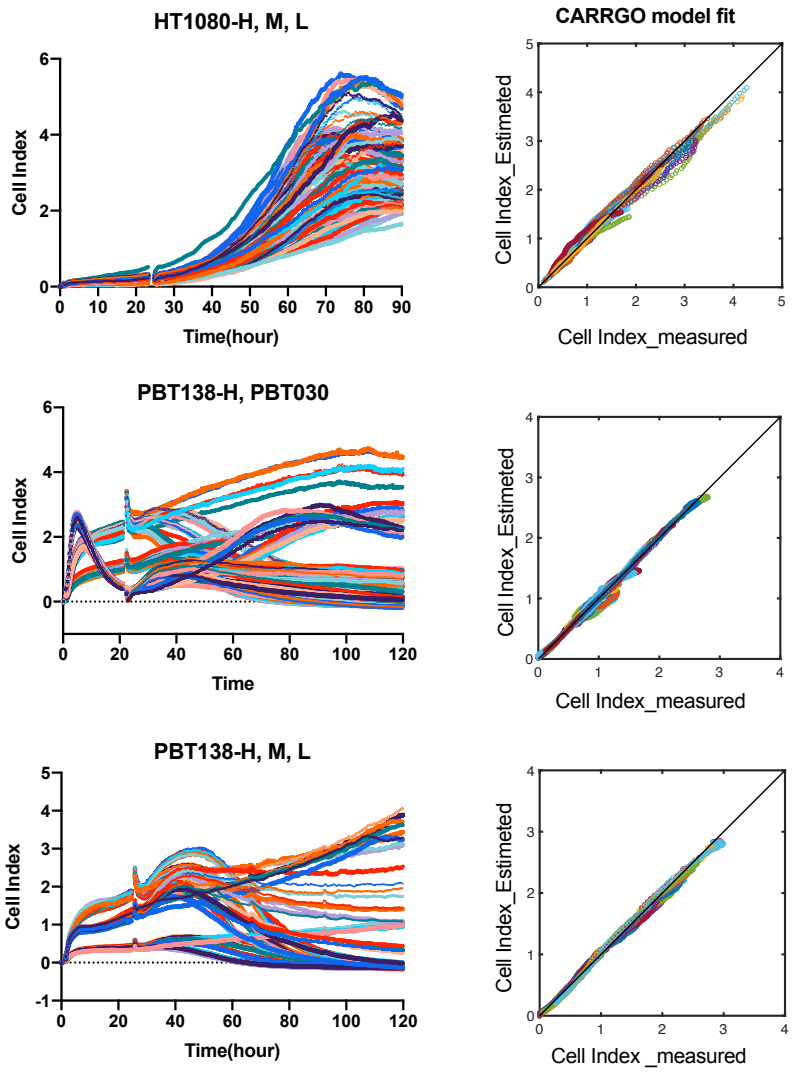

Figure S3. **CAR T cell killing kinetics as measured by xCELLigence.** (Left column) IL13Rα2 CAR T-cells and cancer cell lines with varying IL13Rα2 antigen expression showing cancer cell dynamics in the 96 well E-plate measured by xCELLigence. (a) HT1080-IL13Rα2 lines engineered for low, med, and high receptor expression. (b) PBT030, a glioma line that endogenously expresses IL13Rα2, and PBT138 a glioma line that does not express IL13Rα2 endogenously (c) PBT138-IL13Rα2 lines engineered for low, med and high receptor expression. Cells were either left untreated (triplicates per cell line) or treated with CAR T-cells with effector to target ratios of 1:5, 1:10, and 1:20. Each cell line was treated with three CAR T-cells: BBζ, 28ζ, and mock. (Right column) Correlation between measured data (X-axis) and CARRGO model estimated data (Y-axis) with R^2=0.9±0.1 (middle row; PBT138-H, PBT030). Data before 24 hours is attachment and spreading phase and not included in the CARRGO model fitting (c.f. Figure 2). Each color represents data from a single well in a 96 well plate (rows).

Partial differential equation model of cell attachment and spreading

We assume that the attachment of cell into the bottom of the well is a diffusion process. **Reaction–diffusion systems** are mathematical models which correspond to change of concentration of substances in space and time. Change in concentration of cancer cell population (C) can be written as

Where D is the diffusion coefficient (mm^2/time), ρ is the net growth rate (1/time) of cancer cells, K is the cancer cell carrying capacity (cells or CI).

$$\overbrace{\frac{\partial C}{\partial t}}^{\substack{rate\ of\ change\ of \\ cancer\ cell\ population}} = \overbrace{\frac{\partial}{\partial x}\cdot\left(D\frac{\partial}{\partial x}C\right)}^{\substack{Dispersion\ of\ cells\ on \\ bottom\ of\ the\ well}} + \overbrace{\rho C\left(1-\frac{C}{K}\right)}^{Logistic\ growth}$$

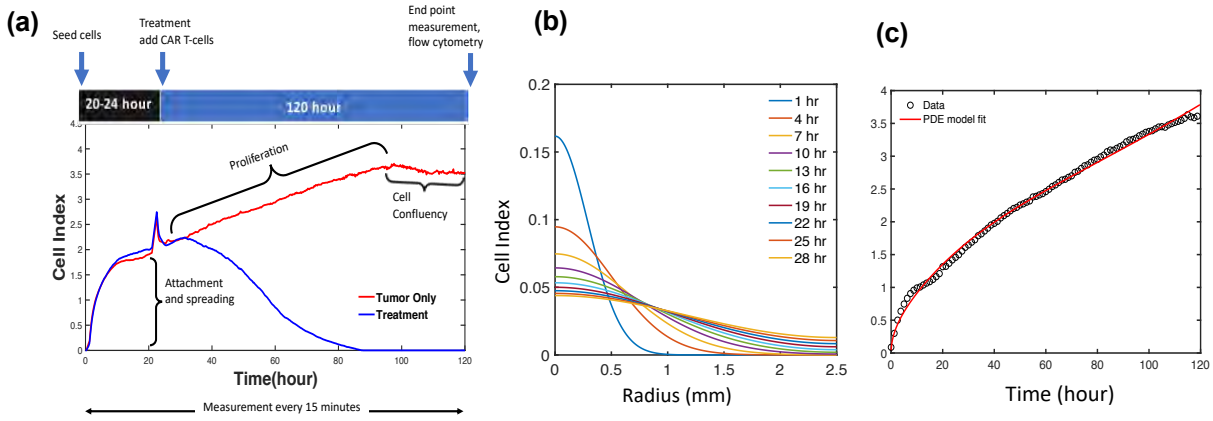

Figure S4. Partial differential equation model of attachment and spreading in xCELLigence system. Initial phase of cancer cell dynamics in the experimental system (a), explaining the attachment and spreading of the cells on the bottom of the plate. (b) solutions of the PDE model showing spatial distribution of cells over time with a point-source (Dirac delta function centered at x=0) initial condition at time t=0, (c) Reaction-diffusion model fitting to the tumor only growth curve data. A diffusion rate D = 0.01 mm^2/hour was used in fitting the reaction-diffusion PDE model to the data. The PDE model fits the attachment and spreading dynamics remarkably well. Because the cell populations are well mixed (Figure S1) we neglect the spatial term in the CARRGO model once the diffusion process is near steady state ($\frac{\partial^2 C}{\partial x^2} \approx 0$, t ~ 24 hours). We show the PDE model fit to this early attachment and spreading phase data for the reader's interest and information.

Sensitivity of CARRGO model fitting to temporal frequency

To investigate the stability of the CARRGO model parameters, we varied the temporal resolution of the data by down-sampling. Data was down-sampled by taking data points in time intervals ranging from 15 minutes (full data) to 10 hours. Top row shows the value of the parameters κ_1, κ_2 and θ for all down-sampled data of a single well. $\kappa_1 = 0.18 \pm 0.003$, $\kappa_2 = 0.08 \pm 0.0005$ and $\theta = 0.001 \pm 2.5 \times 10^{-6}$. Repeated measure ANOVA was performed to check the variability in the parameter values at 1 hour, 5 hours, and 10 hours of down-sampled data. No significant difference (p>0.1) was found in the ANOVA test. Bottom row shows the fitting of the model to the data for 1, 5, and 10-hour time intervals. The CARRGO model fit well to all down-sampled data with $R^2 \approx 0.9$, indicating consistency and reproducibility of the model and the data.

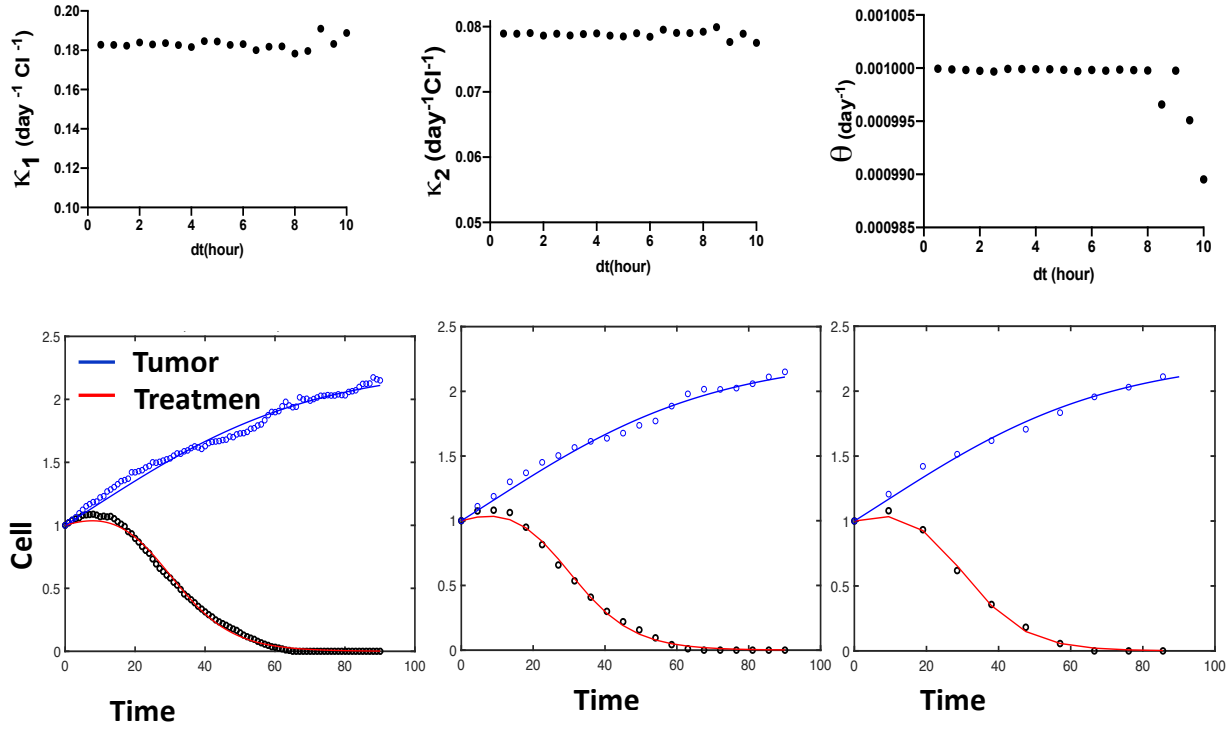

Figure S5. Effect of data sampling on CARRGO model parameter estimates. Top row shows the value of the parameters κ_1, κ_2 and θ for all down-sampled data of a single well for cell line PBT138-H treated at dose E:T=1:5. Bottom row shows the fitting of the model to the data of 1, 5, and 10 hour time intervals.

Sensitivity of CARRGO model fitting to the end time of measured data point

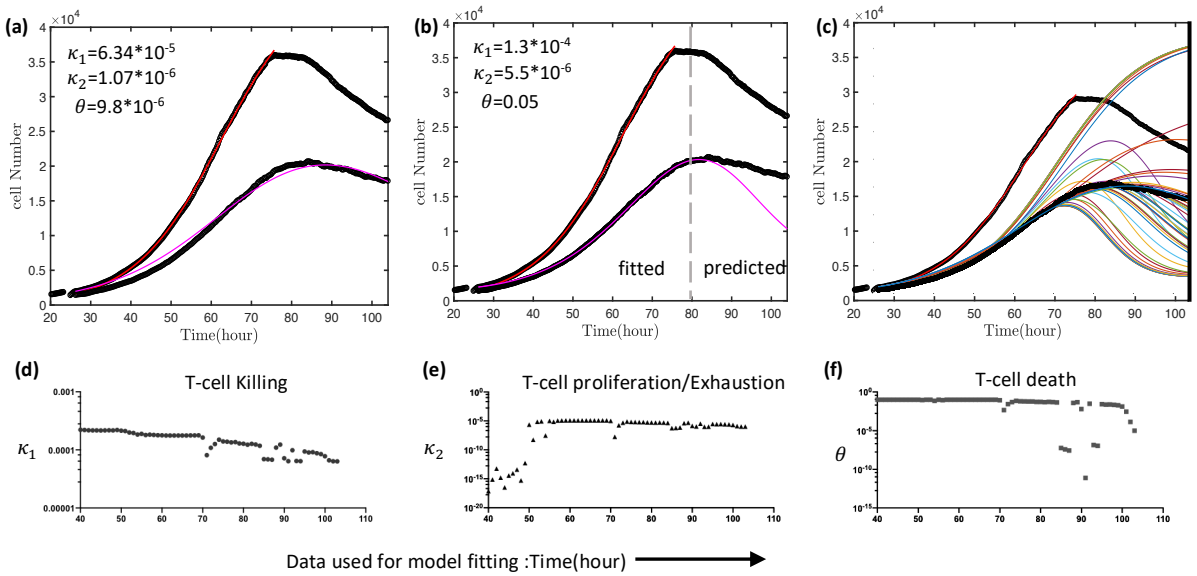

Figure S6. **Sensitivity of CARRGO model fitting and prediction to the end time of measured data point.** (a) CARRGO model fitting when the full time series of data was used. (b) CARRGO model fitted for only for 80 hour and dynamics for later time points are predicted. (c) The model predicted dynamics when fewer time series data are used for model fitting and corresponding κ_1, κ_2, θ values are shown in (d), (e), (f) respectively. This suggests κ_2 is the most sensitive parameter to predict the tumor dynamics.

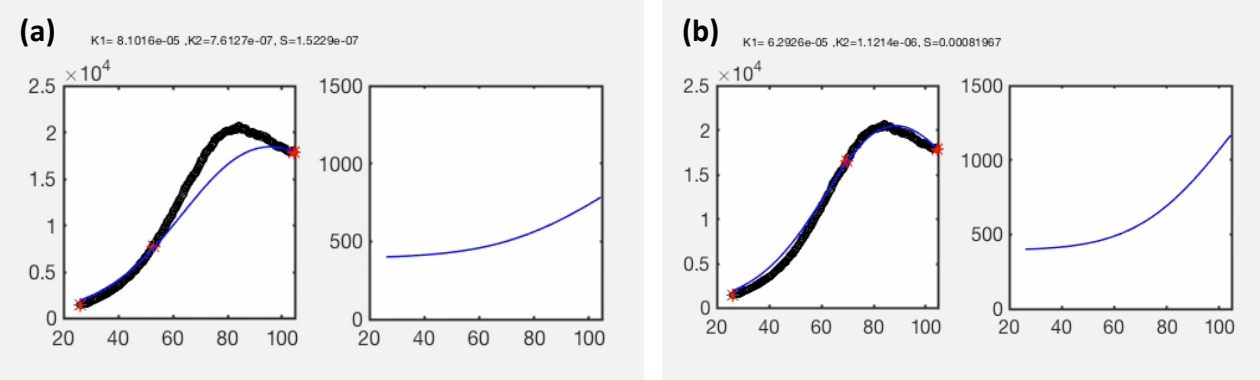

Movie S1. **CARRGO model fit to only three data points.** Because there are three treatment-related parameters in the CARRGO model, three is the minimum number of data points needed to identify these parameters. We examined the sensitivity of parameter identification by using the initial (t=24 hours post seeding) and final time points and varied the third time point. (Left plot) Black points are raw xCELLigence data for HT1080-H treated with 1:5 effector to target ratio BBζ CAR T-cells. Red asterisks are data used to fit CARRGO model. Blue curve is CARRGO model solution. (Right plot) CARRGO predicted CAR T-cell population. (a) Third data point at t = 50 hours. (b) Third data point at t = 70 hours. The best fit to the whole data occurs when the third point lies between the growth curve inflection point (t~65 hours) and maximum (t~80 hours). We include a movie which shows the effect of varying the third data point from t = 24 to t = 110 hours.

Simulation to test uniqueness of CARRGO model parameters

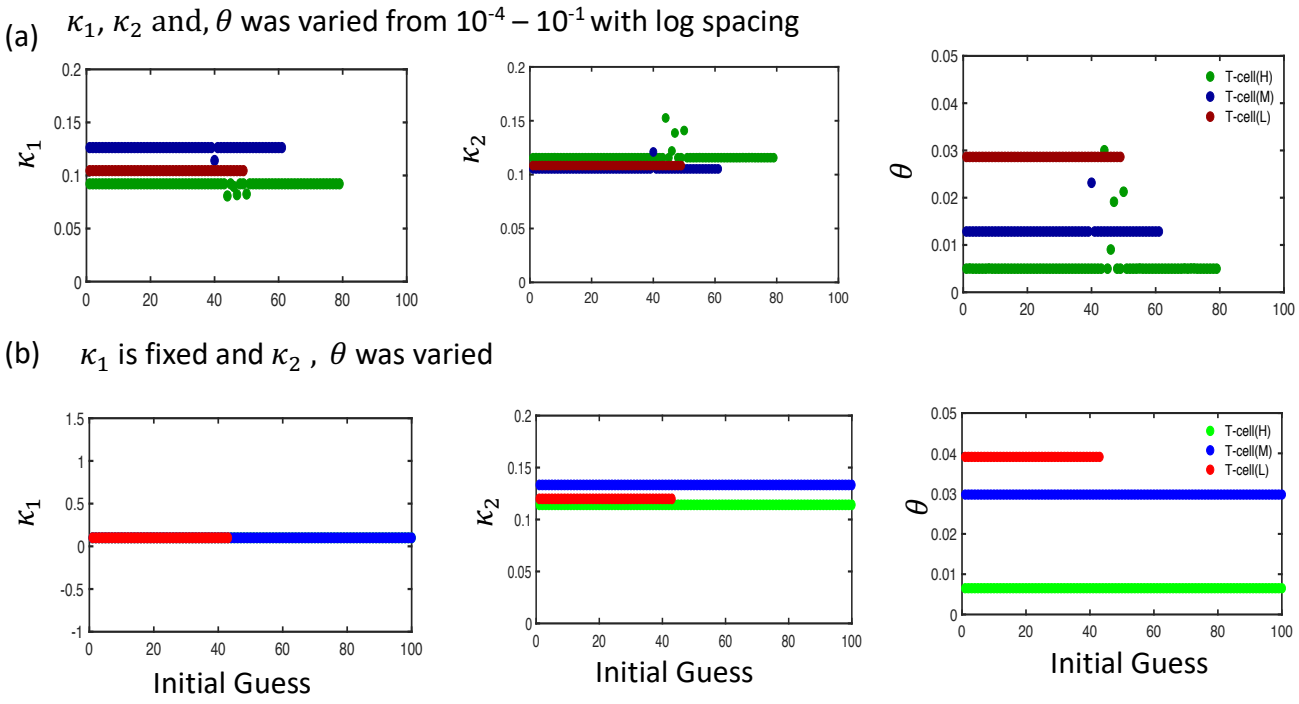

Figure S7. Simulation to test uniqueness of CARRGO model parameters. Uniqueness of the parameters was tested by choosing 100 different combinations of values of the parameters across several orders of magnitude for the model fitting optimization procedure. We found that if the optimization converged, it converged to unique values of the parameters. Top row shows the converged parameter values started from 100 different combination initial guess in parameter ranges from 10^{-4} – 10^{-1} with log spacing and 300 iterations. Except for a few points, the model converges to unique set of parameters. Those points again converge to the unique solution when number of iterations is increased. Bottom row shows the convergence of the model when one of the parameters is fixed. With a constrained variable, the optimization converged to a unique set of parameters with fewer iterations. Since the value for θ was very small, we constrained θ for all CARRGO data fitting.

SUPPLEMENTARY DATA 2 (Figs. S8-S11)

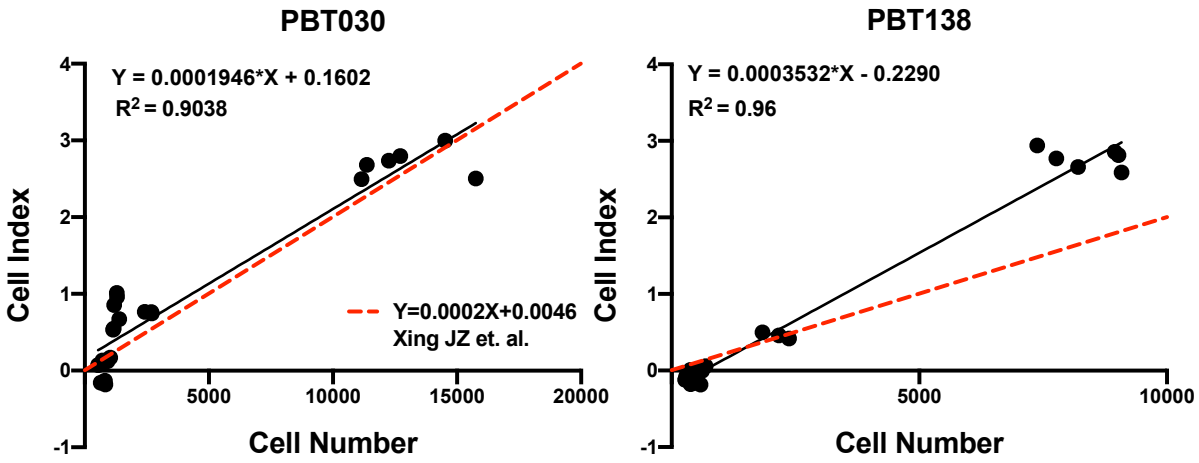

Figure S8. Linear relation between cell index (CI) and cell number (CN). A strong linear relationship exists between the xCELLigence output of cell Index and the total number of cells in the well. Data is shown for cell lines PBT030 and PBT138-H. Cell numbers were measured with flow cytometry at 120 hours after cell seeding at the end of the experiment. Measurements were taken from all wells in the 96 well plate with seeding densities 12.5k. The red line shows the slope of published report by Xing et al. (1).

Because the xCELLigence system is an indirect measure of cell number, we validated previously published relationships between cell number and the output of the xCELLigence system, Cell Index (CI) by performing flow cytometry at the end of the experiments. The strong correlation ($R^2 > 0.90$) and slope is consistent with previously published reports (1). The linear relation between cell index and cell number has been confirmed by many authors, however, the slope is very much cell line dependent(1,2).

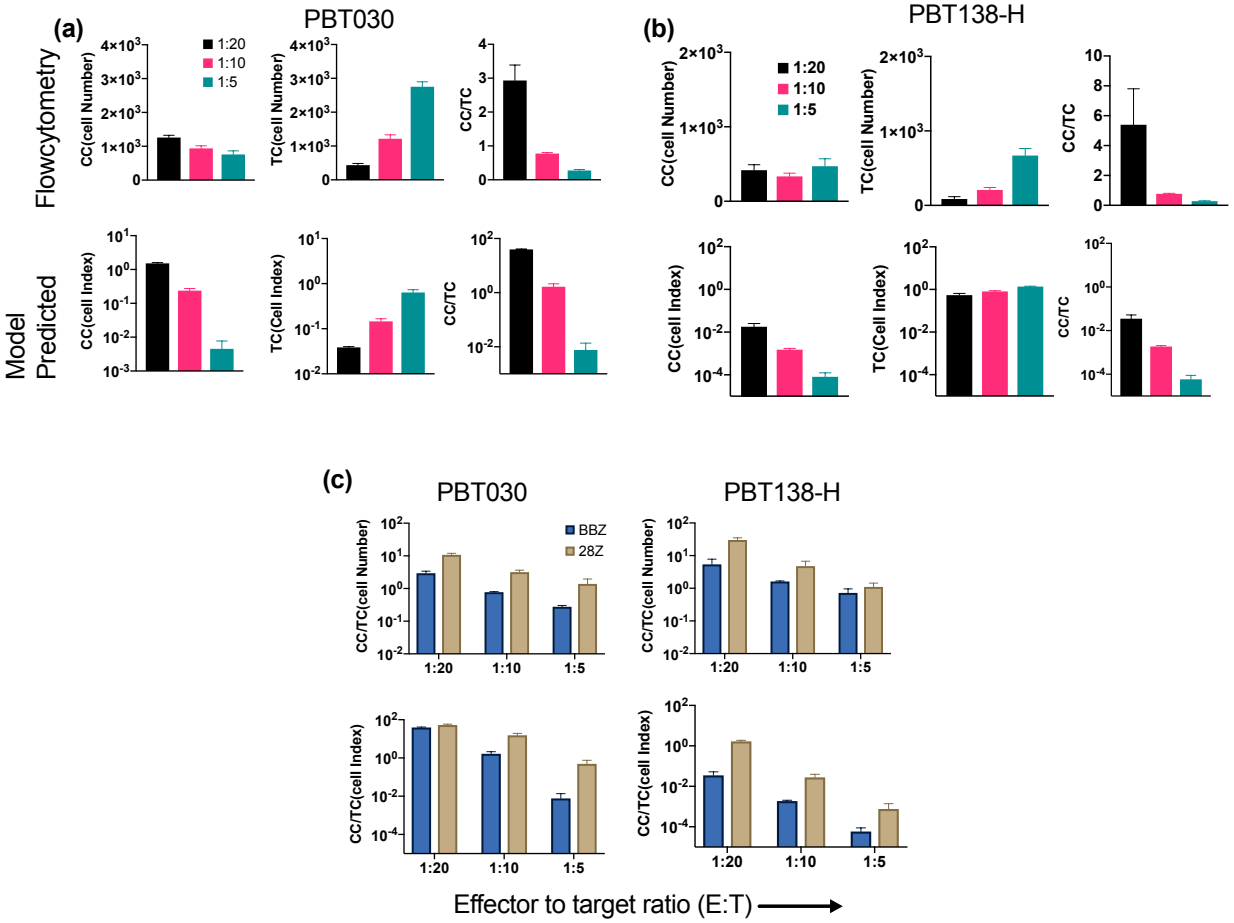

Figure S9. Validation of CARRGO predicted cancer cell - CAR T-cell ratio by flow cytometry. Bar plots (a), (b) showing comparison between flow cytometry (top row) and model predicted (bottom row) cancer cell (CC), CAR T-cell (TC) and the ratio CC/TC for cell lines PBT030 and PBT138-H respectively, treated with BBζ CAR T-cells. (c) Bar plot shows cancer cell to T-cell ratio for both cell lines and comparison of BBζ and 28ζ. Note the decreasing trend of CC/TC with respect to CAR T-cell dose observed in flow cytometry is preserved in model predicted CC/TC. Similar trends were observed for both type of CAR T-cells BBζ and 28ζ. However, CC/TC for the cells treated with 28ζ is higher than BBζ indicating BBζ may present superior treatment outcome than 28ζ. This result is consistent with previously published literature (3,4).

Because flow cytometry and the xCELLigence systems are inherently different measurements with different units, we cannot compare them directly. Rather, we observe trends across target to effector ratios and cell lines to validate the CARRGO model predictions.

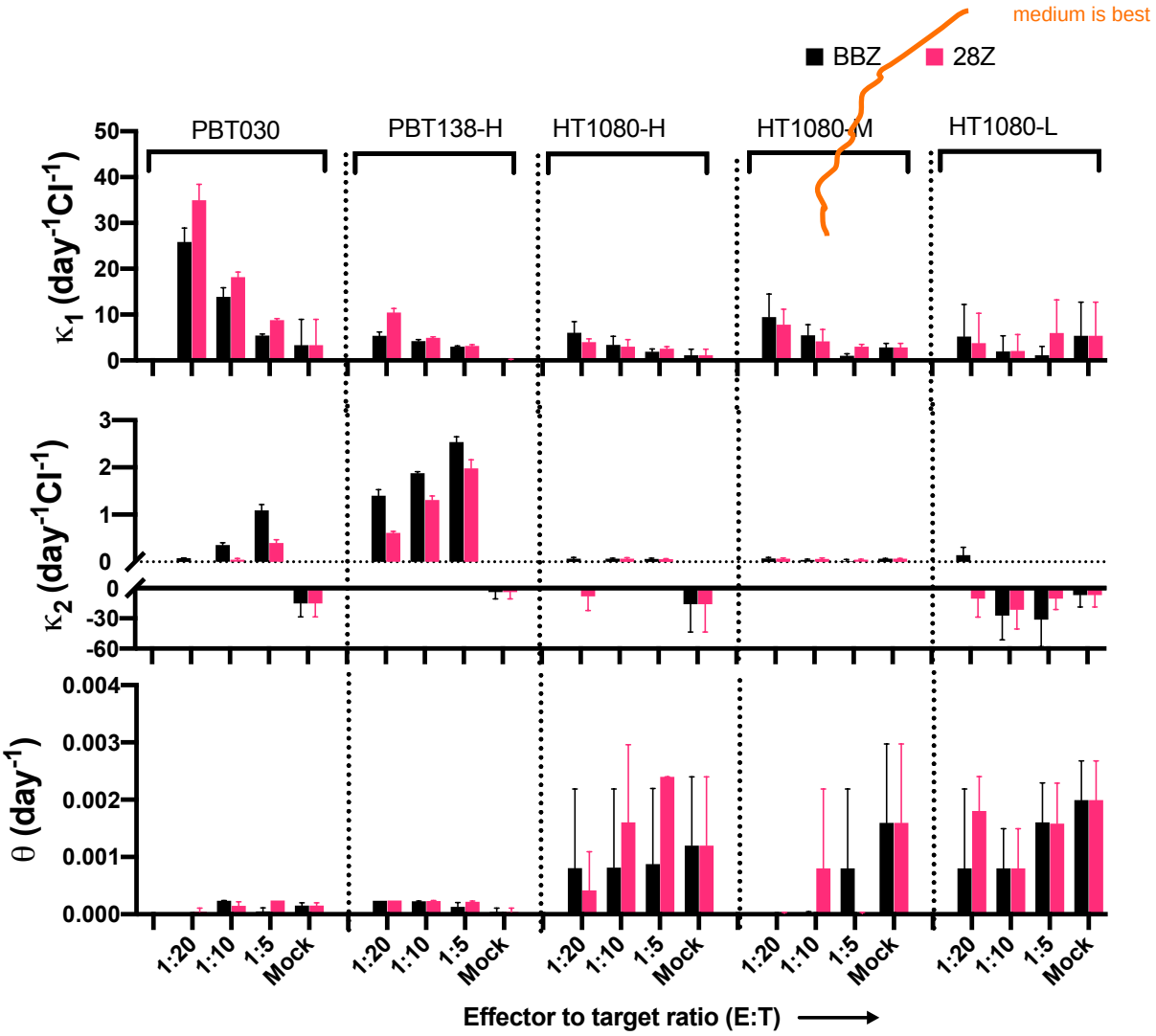

Figure S10. **CARRGO model parameters for different cell lines and comparison between BBζ and 28ζ IL13Rα2-CAR T-cells.** (top row) Bar plots showing killing rate (κ_1), (middle row) exhaustion rate (i.e., loss of effector activity) (κ_2), (bottom row) and net death rate (θ), of PBT030, PBT138-H, and HT1080-H, HT1080-M, HT1080-L with tumor seeding 12.5×10^{-3}, three different effectors to target ratios (1:5, 1:10, 1:20). Black bars are are parameters for cells treated with CAR T-cell BBζ and pink bars for cells treated with 28ζ. κ_1 and κ_2 shows similar trend for both CAR T-cells BBζ and 28 ζ.

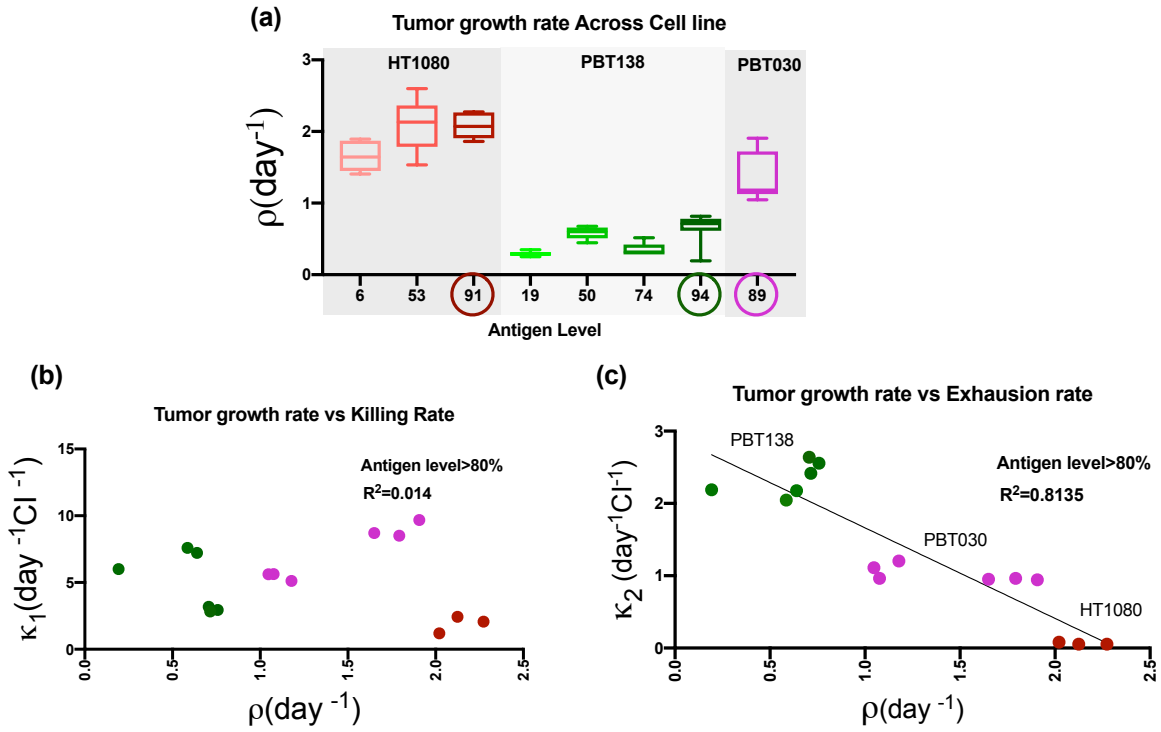

Figure S11. Killing kinetics of CAR T-cells as compared to tumor growth rate. Box plot shows tumor growth rate across cell lines with percentage of antigen expression levels (a). For cell lines with antigen levels >80%, the rate constant κ_2 is negatively correlated with tumor growth rate (b) however, the killing rate κ_1 did not show any significant correlation with tumor growth rate. As we see in (a) tumor growth rate could also vary with antigen level, we only take cell lines with antigen level more than 80% to see the correlation of tumor growth and κ_1, κ_2.

REFERENCES

1. Xing JZ, Zhu L, Gabos S, Xie L. Microelectronic cell sensor assay for detection of cytotoxicity and prediction of acute toxicity. Toxicol Vitr. 2006 Sep 1;20(6):995–1004.

2. Chiu C-H, Lei KF, Yeh W-L, Chen P, Chan Y-S, Hsu K-Y, et al. Comparison between xCELLigence biosensor technology and conventional cell culture system for real-time monitoring human tenocytes proliferation and drugs cytotoxicity screening. J Orthop Surg Res. 2017 Oct 16;12(1):149.

3. Zhong Q, Zhu Y, Zheng L, Shen H, Ou R, Liu Z, et al. Chimeric Antigen Receptor-T Cells with 4-1BB Co-Stimulatory Domain Present a Superior Treatment Outcome than Those with CD28 Domain Based on Bioinformatics. Acta Haematol. 2018;140(3):131–40.

4. Milone MC, OConnor R, May M, Albelda S, Philipson B. 4-1BB-Costimulated CAR-Mediated Non-Canonical NF-Kb Signaling Enhances CAR T Cell Survival and Suppresses Bim Expression. Blood. 2018 Nov 21;132(Suppl 1):3713–3713.

STRUCTURAL IDENTIFIABILITY ANALYSIS OF CARRGO MODEL

$$\frac{dX}{dt} = \rho X(1 - \frac{X}{K}) - \kappa_1 XY \tag{1}$$

$$\frac{dY}{dt} = \kappa_2 XY - \theta Y \tag{2}$$

Let us examine the structural identifiability of the model with unknown parameters $\{\kappa_1, \kappa_2, \theta\}$ and observable quantities $\{X(t,p) = X, Y(t,p) = Y\}$. We assume that the parameters ρ and K are known as well as the initial condition values. We will attempt to compute this using Taylor series approach and generating series approach.

The Taylor series approach assumes that the observation functions are analytic in a neighborhood of $t = 0$, and the their successive time derivatives are measurable and contain information about the parameters to be identified. Using the measurable quantities at the successive time as $t = 0^+$. The problem reduces to determining the number of solutions for the parameters in a set of algebraic equations. From the system equations, we have

$$\begin{aligned} X'(0^+) &= \rho X(0^+)(1 - \frac{X(0^+)}{K}) - \kappa_1 X(0^+)Y(0^+) \\ Y'(0^+) &= \kappa_2 X(0^+)Y(0^+) - \theta Y(0^+). \end{aligned}$$

Be denoting the measurable initial quantities as $X_0 = X(0^+)$, $X_1 = X'(0^+)$, $Y_0 = Y(0^+)$, $Y_1 = Y'(0^+)$, we have

$$\begin{aligned} X_1 &= \rho X_0(1 - \frac{X_0}{K}) - \kappa_1 X_0 Y_0, \\ \kappa_1 &= \frac{\rho}{Y_0}(1 - \frac{X_0}{K}) - \frac{X_1}{X_0 Y_0}, \end{aligned}$$

so that κ_1 is structurally identifiable. For the other parameters, we consider an additional derivative as $Y'' = \kappa_2 X'Y + \kappa_2 XY' - \theta Y'$, and measurable $Y_2 = Y''(0^+)$. We have

$$\begin{aligned} Y_1 &= \kappa_2 X_0 Y_0 - \theta Y_0 \\ Y_2 &= \kappa_2(X_1 Y_0 + X_0 Y_1) - \theta Y_1, \end{aligned}$$

so that we can solve for the remaining parameters as

$$\kappa_2 = \frac{-Y_1^2 + Y_0 Y_2}{X_1 Y_0^2}, \qquad \theta = \frac{X_0 Y_0 Y_2 - X_1 Y_0 Y_1 - X_0 Y_1^2}{X_1 Y_0^2}.$$

Date: September 27, 2019.

Therefore, the variables $\{\kappa_1, \kappa_2, \theta\}$ are structurally identifiable except at most a set of points of zero measure, that is, points for $X_0 = 0, Y_0 = 0, X_1 = 0$. In addition, the generating series approach using the MATLAB library GENSSI computes three Lie derivatives and verifies that $\{\kappa_1, \kappa_2, \theta\}$ are structurally locally identifiable.